



## Preparation and Characterization of some Composite Phosphate Glass-Polyaniline Derivatives Studying Their Antimicrobial Activity



CrossMark

A. Kh. Helmy<sup>a\*</sup>, H. A. ElBatal<sup>a</sup>, F.H.ElBatal<sup>a</sup>, M. A. Ouis<sup>a</sup>, A. A. Gamal<sup>b</sup>, H. M. Abd El-Salam<sup>c</sup>

<sup>a</sup> Glass Research Department, National Research Centre, Dokki, Cairo, Egypt

<sup>b</sup> Chemistry of Natural and Microbial Products Department, National Research Centre, Dokki, Cairo, Egypt

<sup>c</sup> Chemistry department, Faculty of Science, Beni-Suef University Beni Suef 62514, Egypt

### Abstract

The present work involved the preparation of mixed composite derivatives from phosphate glass and polyaniline together with additional doped samples containing increasing CuO or ZnO (3→10 mol%). All prepared pure glass and polyaniline together with their composites were characterized by structural FTIR analysis, X-ray diffraction examinations and surface scanning electron microscope (SEM). Further antimicrobial properties of the base glass, base polyaniline and composites with one of the two dopants (CuO,ZnO) were studied and evaluated. FT infrared spectrum of the base undoped glass revealed vibrational bands due to PO<sub>4</sub> tetrahedral groups which are extended from 400 cm<sup>-1</sup> to 1500 cm<sup>-1</sup> within the mid region. The base polyaniline exhibits extended vibrational bands characteristic for vibrations of C - C, C - H, C = C and N - H groupings. The composite (glass + polyaniline) showed mixed or interfering vibrations of all constitutional groupings. The dopant oxides showed only limited variations to the IR spectra. X-ray diffraction patterns of base and doped glass samples revealed only undefined humps with no indication for crystalline species but only amorphous structures. On the other hand, polyaniline revealed two diffraction peaks which were correlated with crystalline components of the polymerized granular texture of the (PANI). SEM investigations revealed mostly amorphous texture for the parent glass and its derivatives but the polyaniline exhibited granular texture which extended to all composites in different forms. Glass and polyaniline composites showed varying responses to micro-organisms. In general, the composites showed favourable data.

*Key words: phosphate glass; polyaniline; FTIR; X-ray; SEM; antimicrobial.*

### 1. Introduction

It has been recognized that the composite matrices fabrication from both glasses and polymers produces desirable mixed candidates for applications as anti-microbial or as biomaterials candidates [1-3]. One of the privilege characteristics of these composites is the amorphous or non-periodic internal structures or polymeric textures.

Glasses have a wide range of variability in chemical compositions with the possibility of including any of more than 50 elements from the periodic table and can thus be available for the needed chemical, mechanical, thermal, and optical

properties [4, 5] and with unlimited fabrication.

Several polymers (natural and synthetic) are suitable for many biomedical applications [1, 6]. Natural polymers offer the convenience of recognition from the biological system because of their similar macro molecular structure to tissues. This further leads to avoid issues related to toxicity and chronic inflammatory reaction stimulation, as well as back of recognition by cells that are frequently provoked by many types of synthetic polymers.

Synthetic polymers represent the largest sector of biodegradable polymers and they can be prepared

\*Corresponding author e-mail: [ahmedelshereef3@gmail.com](mailto:ahmedelshereef3@gmail.com); (Ahmed Helmy).

Receive Date: 13 June 2021, Revise Date: 29 June 2021, Accept Date: 04 July 2021

DOI: 10.21608/EJCHEM.2021.80482.3986

©2021 National Information and Documentation Center (NIDOC)

under controlled conditions. They exhibit, in general, reproducible and predictable mechanical and physical properties.

The other partner component of the desired studied composite in this work is a specific polymer of polyaniline. In last decades, conducting synthetic polymers have been studied because of their wide applications in many fields such as thin film transistors, super-capacitors, batteries, chemical sensors, activators, electromagnetic shielding and antibacterial agent [7, 8].

Among the conducting polymers, polyaniline (PANI) shows high conductivity and thermal stability because of its conjugated backbone. Delocalization of  $\pi$  electron along their polymeric backbone gives them unique optical and electrical properties [8]. Also, polymer was used as coating for protecting the oxidizable metals from corrosion [9-11]. Using polyaniline in bio-applications is often limited because it is insoluble in common laboratory solvents, hence making it difficult to be processed. The insolubility of (PANI) in most common solvents can be overcome to some extent, by co-polymerizing aniline with substituents that impart solubility to the resulting functionalized aniline-based polymers [12]. The antibacterial effect of conducting polyaniline has been studied with different bacterial strains, and high activity was observed for potential application in the designing of medical clothing like antibacterial fabrics [13]. Broad spectrum antimicrobial activity of substituted polyaniline has an antibiotic resistance against gram negative and gram positive bacteria so, they could be useful for medical devices and food packaging [14].

The main objective of the present study is to investigate the structural FTIR spectral properties of the prepared phosphate glass sample, prepared polyaniline and their mixed composites containing added dopants of either CuO or ZnO (3→10 mol%) together with their antibacterial affinities. The work is extended to investigate the surface texture by scanning electron microscope (SEM) measurements for the basic constituents (host glass-polyaniline) and some selected mixed composites with the addition of one of selected dopant oxides (CuO, ZnO) and compare their morphological and textural properties.

## 2. Experimental details

### 2.1. Preparation of the glasses

The main chemical compositions of the studied phosphate glasses are (P<sub>2</sub>O<sub>5</sub> 50 mol%- K<sub>2</sub>O 30 mol%- CaO (20-X) mol%) where X is CuO or ZnO with various ratios as shown in Table (1). The glasses were prepared from chemically pure materials including ammonium dihydrogen orthophosphate (NH<sub>4</sub>H<sub>2</sub>PO<sub>4</sub>) as a source of P<sub>2</sub>O<sub>5</sub>, the alkali oxide

(K<sub>2</sub>O) was introduced in its respective anhydrous carbonate (K<sub>2</sub>CO<sub>3</sub>) and the same for alkaline earth oxide CaO added in form of (CaCO<sub>3</sub>) while copper and zinc ions were introduced as their respective oxides directly (CuO, ZnO).

The weighed batches were melted in covered porcelain crucibles. The melting was carried out in electric furnace (Vecstar, UK) at 500°C at first to expel ammonia and water vapour and then the temperature was raised and fixed at 1000°C for 60 minutes with frequent rotating the crucibles at intervals to promote homogeneity and complete mixing. The melts were poured on slightly warmed stainless steel molds and the prepared samples were immediately transferred to a muffle regulated at 285°C. Then the annealing muffle was left to cool after 1 hour to room temperature.

Table (1) Codes of the prepared samples

(P <sub>2</sub> O <sub>5</sub> 50 mol%- K <sub>2</sub> O 30 mol%-CaO 20mol%)	Base Glass
(P <sub>2</sub> O <sub>5</sub> 50 mol%- K <sub>2</sub> O 30 mol%-CaO 17 mol%-3 CuO mol%)	3 Cu Glass
(P <sub>2</sub> O <sub>5</sub> 50 mol%- K <sub>2</sub> O 30 mol%-CaO 15 mol%-5 CuO mol%)	5 Cu Glass
(P <sub>2</sub> O <sub>5</sub> 50 mol%- K <sub>2</sub> O 30 mol%-CaO 13 mol%-7 CuO mol%)	7 Cu Glass
(P <sub>2</sub> O <sub>5</sub> 50 mol%- K <sub>2</sub> O 30 mol%-CaO 10 mol%-10 CuO mol%)	10 Cu Glass
(P <sub>2</sub> O <sub>5</sub> 50 mol%- K <sub>2</sub> O 30 mol%-CaO 17 mol%-3 ZnO mol%)	3 Zn Glass
(P <sub>2</sub> O <sub>5</sub> 50 mol%- K <sub>2</sub> O 30 mol%-CaO 15 mol%-5 ZnO mol%)	5 Zn Glass
(P <sub>2</sub> O <sub>5</sub> 50 mol%- K <sub>2</sub> O 30 mol%-CaO 13 mol%-7 ZnO mol%)	7 Zn Glass
(P <sub>2</sub> O <sub>5</sub> 50 mol%- K <sub>2</sub> O 30 mol%-CaO 10 mol%-10 ZnO mol%)	10 Zn Glass
Composite (Polyaniline containing Base glass)	Base Comp
Composite (Polyaniline containing 3 Cu glass)	3 Cu Comp
Composite (Polyaniline containing 5 Cu glass)	5 Cu Comp
Composite (Polyaniline containing 7 Cu glass)	7 Cu Comp
Composite (Polyaniline containing 10 Cu glass)	10 Cu Comp
Composite (Polyaniline containing 3 Zn glass)	3 Zn Comp
Composite (Polyaniline containing 5 Zn glass)	5 Zn Comp
Composite (Polyaniline containing 7 Zn glass)	7 Zn Comp
Composite (Polyaniline containing 10 Zn glass)	10 Zn Comp

### 2.2. Preparation of polyaniline

5 ml of liquid aniline monomer in acidic medium (HCl / 1.25 M) was polymerized by oxidation to polyaniline using potassium dichromate solution (K<sub>2</sub>Cr<sub>2</sub>O<sub>7</sub> / 0.44 M) as an oxidant. The formed precipitate was washed by distilled water and dried in autoclave at 70°C for two hours.

### 2.3. Preparation of the composite (glass+polyaniline)

The adopted method for the preparation of the

glass/polymer composite involves the following steps:

- 5 gm of phosphate glass was grounded to fine powder and dissolved in distilled water
- 5 ml of aniline monomer was added to the prepared solution.
- Few drops of HCl (1.25 M) were added to the mixed solution.
- Addition of 15 ml of the oxidant solution ( $K_2Cr_2O_7$ ) with the required concentration (0.44 M).
- Polymerization process occurred overnight at about 4°C.
- Filtration and washing of the formed precipitate by distilled water.
- Drying the precipitate for 2 hours at about 70°C to get rid of any moisture.

#### 2.4. FTIR spectral studies

Structural analysis of the basic primary constituents of the base glass, polyaniline and their composites were carried out using FTIR spectral measurements. A recording spectrometer (type Bruker VERTEX 80v, Germany) was used covering the wave number range 400-4000  $cm^{-1}$  with a resolution of 4  $cm^{-1}$ .

#### 2.5. X-ray diffraction analysis

X-ray diffraction (XRD) analysis of powders of the prepared samples was carried out at room temperature (RT) with an Empyrean diffractometer by Panalytical (Almelo, The Netherlands), using Cu X-ray tube operated at 30 mA and 45 kV, and using a Ni filter to eliminate  $K\beta$  radiation and a Pixcel3D detector. The diffraction patterns were collected with the step scanning mode in the  $2\theta$  range 5°–80° with step size of 0.03° and counting time of 20 s/step.

#### 2.6. Morphological studies using scanning electron microscopic technique (SEM)

The surfaces textures of the basic constituents of glass, polyaniline and the prepared composites of them together with some selected samples containing dopants of CuO or ZnO were examined by a high resolution scanning electron microscope apparatus SEM model (QUANTA FEG 250 with field emission gun, FEI Company – Netherlands).

#### 2.7. Antimicrobial studies

The base polyaniline, parent glass and their

corresponding composites were shaped in disk forms and impeded on the surface of the bacterial media (nutrient agar) for studying their antimicrobial (antibacterial and antifungal) effects on three indicator microorganisms including gram-positive bacteria (*Staphylococcus aureus*), gram-negative bacteria (*Escherichia Coli*) and yeast (*Candida albicans*) by agar diffusion method (Mishra & Prasad, 2005) [14].

Overnight cultures of the selected organisms were inoculated in nutrient agar media and potato dextrose agar for bacteria and yeast, respectively, and then poured in sterile petri dishes.

The comparative activities of parent glass, polyaniline and composites were investigated besides testing the samples containing 1, 3, 5, 7, 10 mol % CuO or 1, 3, 5, 7, 10 mol % ZnO.

The microorganisms were passaged at least twice to ensure purity and viability. About 0.2 gm of the prepared powder (disk) samples were applied on the inoculated agar plates and incubated for 24 hours at their optimum growth temperature. The antimicrobial effect was evaluated by measuring the inhibition zone diameter around samples (disks) in (cm).

### 3. Results

#### 3.1. FTIR spectral results

Figures (1) illustrates the FTIR spectra of different samples including

- Base glass, base comp and polyaniline
- Pure base glass and all Cu glass samples
- Pure base glass and Zn glass samples
- Base comp and all Cu comp samples
- Base comp and all Zn comp samples

The FTIR spectral features appear quite different and can be described as follows:

##### (a) FTIR spectrum of base phosphate glass

As a whole, the FTIR spectrum (Figure 1) reveals distinct strong vibrational bands with sharp peaks within the mid-range from 400 to 1400  $cm^{-1}$  followed by two successive medium broad bands centered at about 1645 and 3450  $cm^{-1}$ . The distinct sharp peaks within the mid region are at 470, 774, 875, 1096 and 1273  $cm^{-1}$ . FTIR spectral data of glass samples doped with CuO (Cu Glass) and that doped with ZnO (Zn glass) are almost the same as that of the base glass sample as there is no distinct variations in peak positions or intensity.

##### (b) FTIR spectrum of polyaniline

The IR spectral vibrational features of the pure

polyaniline are observed to be extended from 400  $\text{cm}^{-1}$  to the end of measurement at 4000  $\text{cm}^{-1}$ . The IR spectrum includes composite absorption bands sometimes with multiple peaks and the details are summarized as follows:

- a. The far-IR region comprises of a band centered at 510  $\text{cm}^{-1}$ .
- b. The mid IR region comprises of broad bands extending from about 800 to 1600  $\text{cm}^{-1}$  with peaks at 810, 1145, 1248, 1300, 1480, and 1600  $\text{cm}^{-1}$ .
- c. The rest of the IR spectrum includes several broad bands extending from 1600 to 4000  $\text{cm}^{-1}$  with peaks at 2850, 2920, 2975, 3390 and 3650  $\text{cm}^{-1}$ .

**(c) FTIR of the base composite (base glass + polyaniline)**

The collected IR spectrum of the (base comp) appears with IR features including the collective vibrational bands due to glass and polyaniline superimposed and extending from 400-4000  $\text{cm}^{-1}$ . The identified vibrational peaks are as follows: 510, 810, 875, 1130, 1300, 1400, 1483, 1645, 2850, 2925, 2980  $\text{cm}^{-1}$  and a broad peak in the range 3300-3690  $\text{cm}^{-1}$ .

**(d) FTIR of the composite doped with CuO (Cu comp)**

The IR spectral data of the CuO-doped composites can be considered as a combination of the IR spectra of (Cu-glass) and that of polyaniline gathered and obviously overlapped on each other with an obvious shift in the position of some peaks belong to polyaniline. The IR spectrum of Cu comp is observed to be extended from 400 to 4000  $\text{cm}^{-1}$  revealing the main mid features (400-1600  $\text{cm}^{-1}$ ) of base glass sample and polyaniline sample and the second region (1600-4000  $\text{cm}^{-1}$ ) is looking nearer to the polyaniline sample more than base glass sample. The peaks at 875, 1300, 1400  $\text{cm}^{-1}$  are identified in the first mid region (400-1600  $\text{cm}^{-1}$ ). Other peaks in the same mid region at 503, 800, 1130, 1236, 1475 and 1553  $\text{cm}^{-1}$  are shifted from 510, 810, 1145, 1248, 1483 and 1565  $\text{cm}^{-1}$  respectively. The second region of the spectrum reveals several peaks at: 1645, 2860, 2920, and 2970  $\text{cm}^{-1}$  beside a broad peak at 3390 to 3670  $\text{cm}^{-1}$ .

**(e) FTIR spectra of ZnO-doped composites**

The FTIR spectra of ZnO-doped composites are similar to that of the composites containing CuO.

**3.2. X-ray diffraction patterns analysis**

Figure (2) illustrates the X-ray diffraction patterns of the base glass, polyaniline and composite derivatives and the experimental data can be summarized as follows:

- i. X-ray data of the base glass and glassy samples doped with CuO or ZnO reveal only a broad hump without any distinct diffraction peaks.
- ii. The X-ray diffraction of polyaniline shows three distinct peaks at about 28.3  $\theta$ , 40.5  $\theta$  and 44.6  $\theta$  with some other minor peaks.
- iii. The base composite (base glass+ polyaniline) reveals only a single medium diffraction peak at about 44.6  $\theta$ .
- iv. The doped composites derivatives reveal with the addition of either CuO or ZnO the same peaks that appeared in the pure polyaniline with a slight variation in their intensity.

**3.3. Scanning electron microscope analysis (SEM)**

Figure (3) illustrates the SEM images of the studied glass, polyaniline, the corresponding composites and doped derivatives. The identified textures can be summarized as follows:

- i. The texture of the different images of the base glass, CuO-doped and ZnO-doped glass reveal amorphous or clear background.
- ii. The base composite (base glass + polyaniline) image shows small granular texture with some few micro-crystalline species.
- iii. The CuO-doped composite samples (3,5,7,10) reveal the increase of micro-crystalline species.
- iv. The composite samples doped with ZnO show micro-granular matrix or back ground and with the increase of ZnO some microcrystals can be identified.
- v. The SEM image of pure polyaniline exhibits distinct micro-granular texture in all the background.

**3.4. Antibacterial activity data**

Table (2) and Figure (4) summarize the different responses of the bacterial growth against the various studied base glass, base polyaniline and composites together with the effects of adding 1→10 mol% of either CuO or ZnO.

The collected data are summarized as follows:

- (a) Parent glass without adding any antibacterial elements showed a degree of antibacterial effect which increases by increasing the concentration of copper and zinc oxides till specific limit (maximum 7 mol %).
- (b) Polyaniline showed antibacterial effect more than that of the parent glass, but some

samples containing zinc or copper oxides overcome the effect of polyaniline.

- (c) All glass-composite samples recorded the best result compared to the base of pure glass or pure polyaniline.

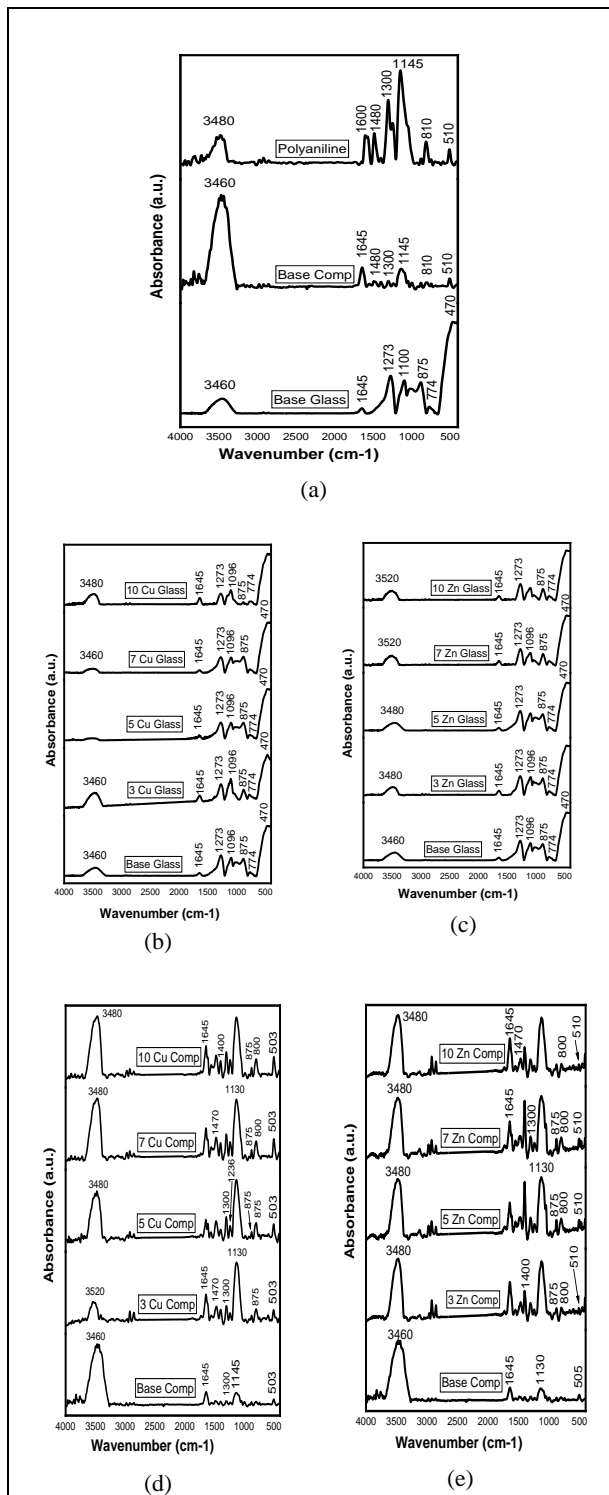


Figure (1) FTIR spectra of (a) base glass, polyaniline, base composite (glass+polyaniline), (b) CuO-doped glasses, (c) ZnO-doped glasses, (d) CuO-doped composites and (e) ZnO-doped composites

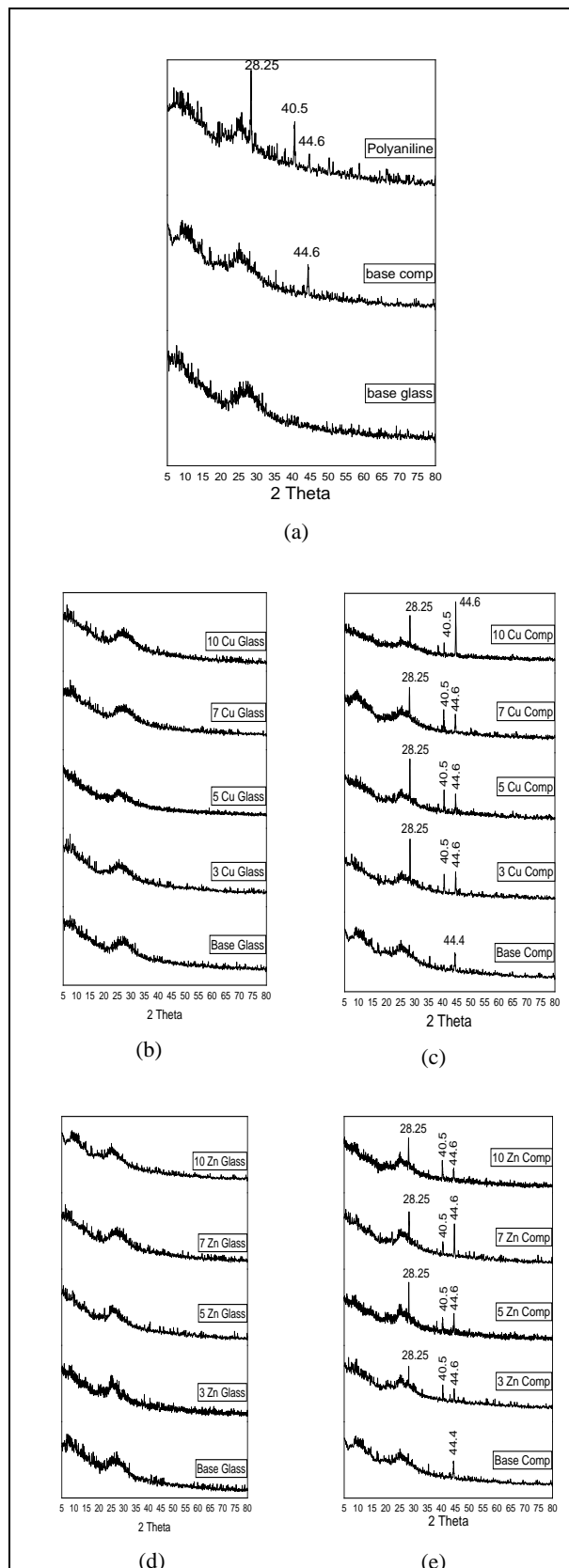
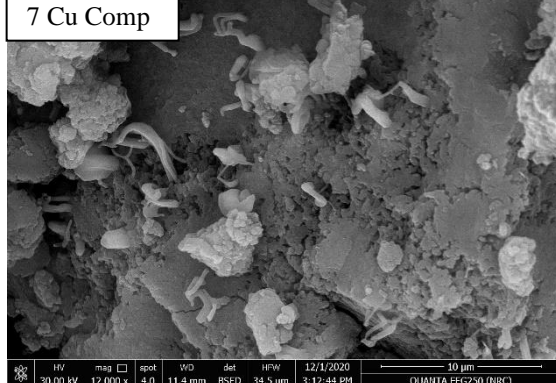
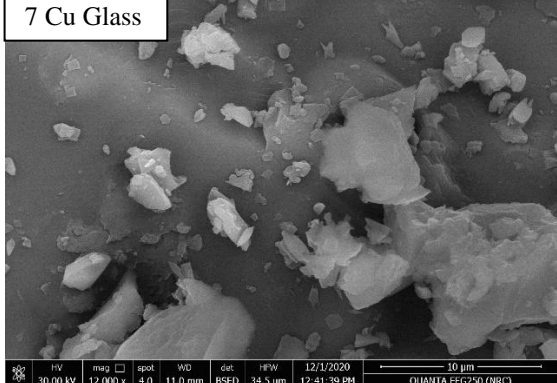
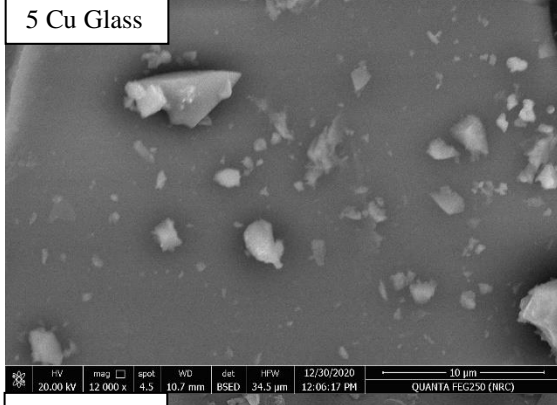
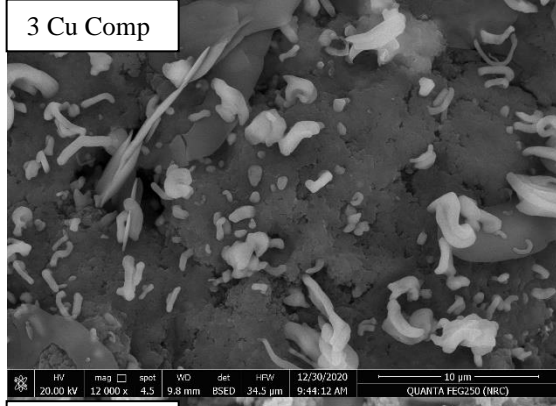
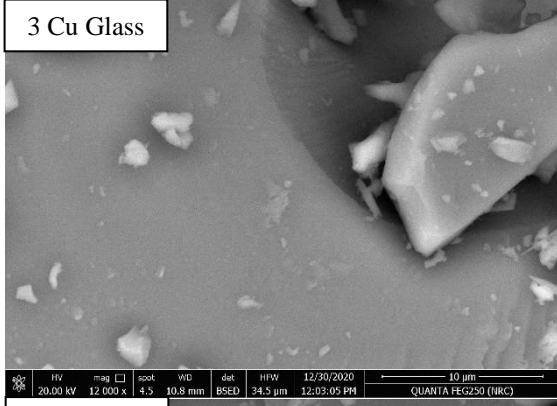
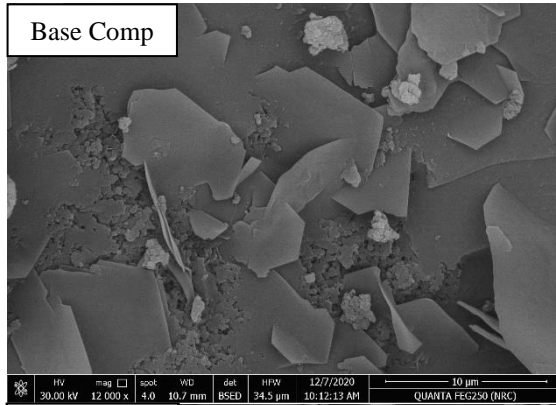
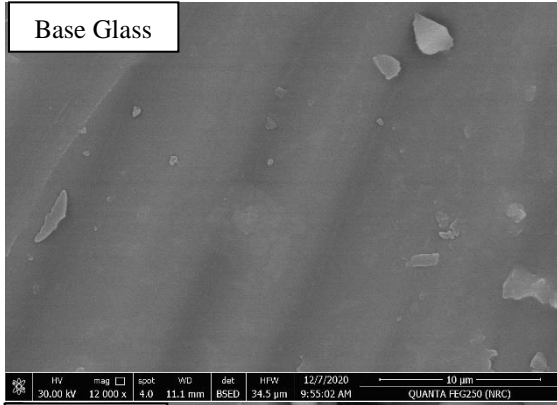
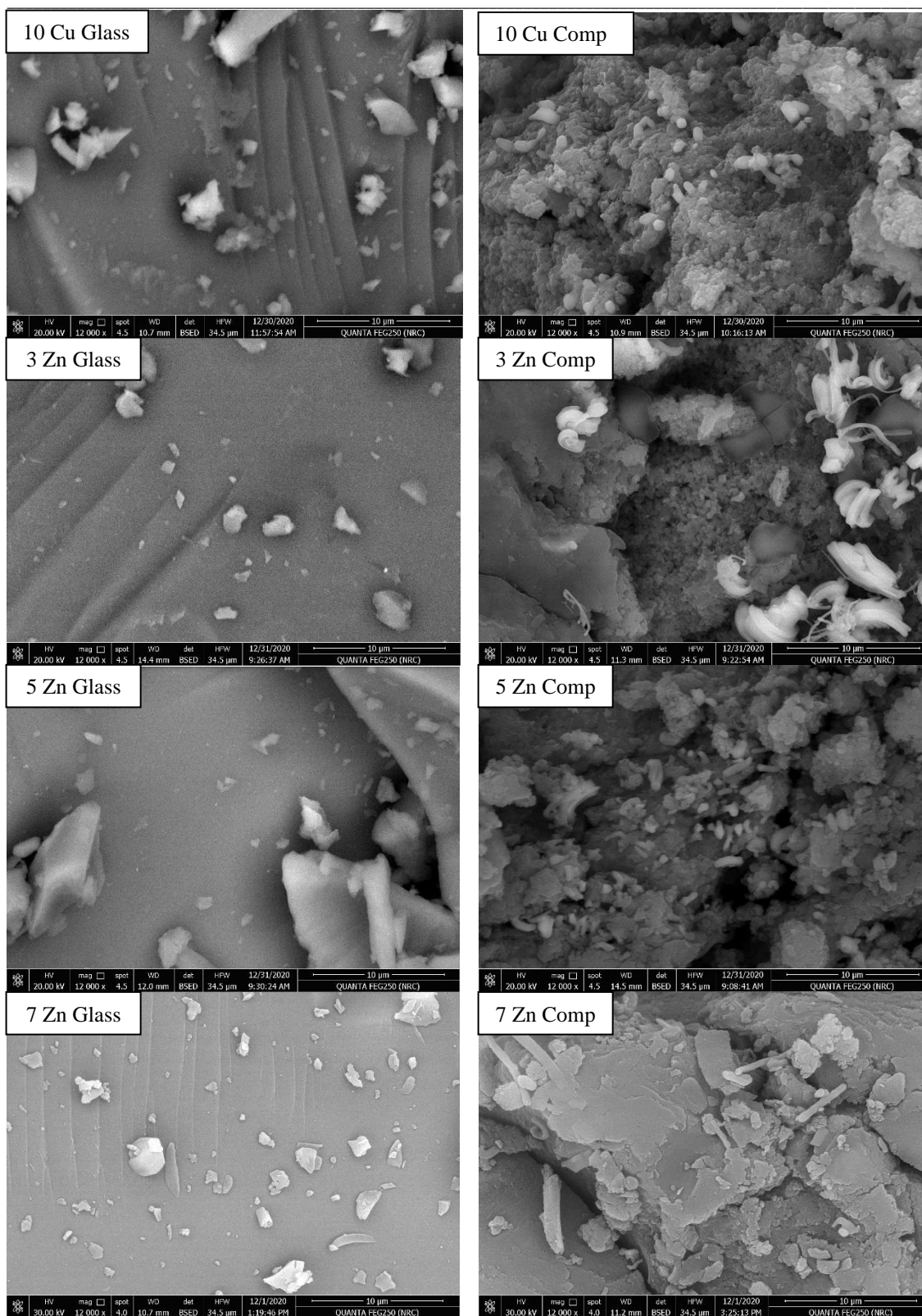


Figure (2) XRD analysis of base glass, polyaniline, base composite (glass+polyaniline), CuO-doped glasses, ZnO-doped glasses, CuO-doped composites and ZnO-doped composites





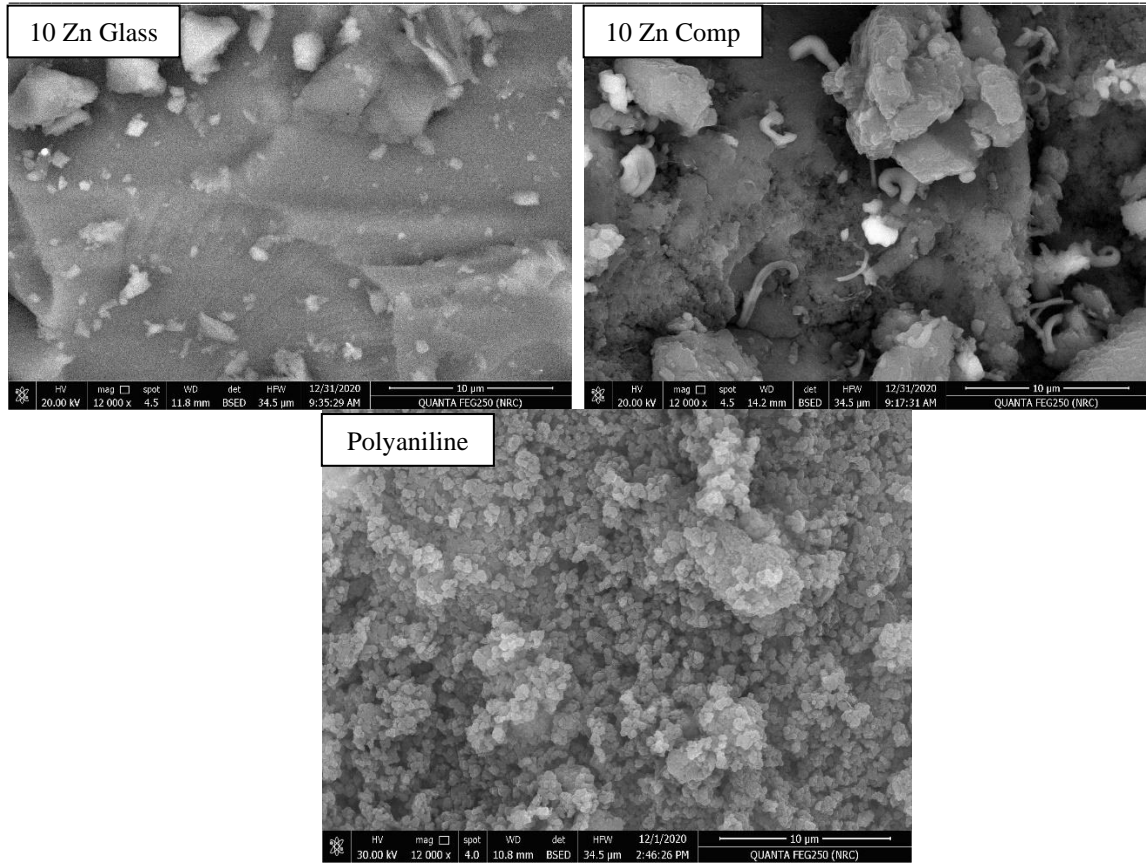


Figure (3) SEM images of the all prepared glass samples, polyaniline and their composites

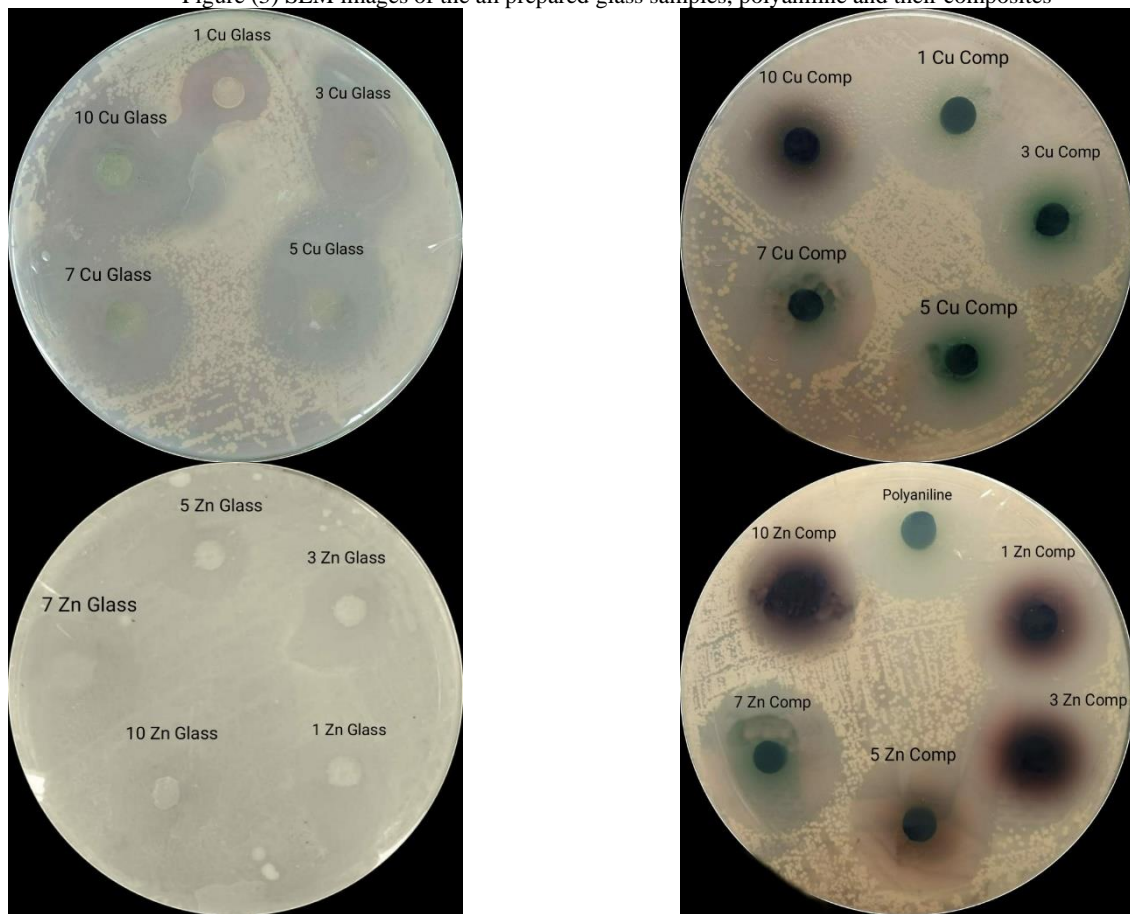


Figure (4) antibacterial petri dishes activities of the prepared samples (glass, polyaniline and their composites) against E.Coli



**Table (2) Antimicrobial activities of glass, polyaniline and their composites**

Sample	Inhibition zone of microbial growth (Cm)		
	Microorganisms		
	<i>Escherichia Coli</i>	<i>Staphylococcus aureus</i>	<i>Candida albicans</i>
1 Cu (Glass)	3.8	3.6	3.4
<u>1 Cu (comp)</u>	4.6	4.5	4.5
3 Cu (Glass)	4.5	4.3	4.2
<u>3 Cu (comp)</u>	4.7	4.7	4
5 Cu (Glass)	4.5	4.4	4.1
<u>5 Cu (comp)</u>	5.1	4.9	4.7
7 Cu (Glass)	5	4.8	4.4
<u>7 Cu (comp)</u>	5.8	5.7	5.7
10 Cu (Glass)	4.8	4.6	4.1
<u>10 Cu (comp)</u>	5.6	5.6	5.5
Base Glass	2.8	2.8	2.7
<u>Base Comp</u>	4.5	4.4	4.2
1 Zn (Glass)	3.2	3.2	3
<u>1 Zn (comp)</u>	4.2	4.1	3.8
3 Zn (Glass)	3.3	3.2	3
<u>3 Zn (comp)</u>	4.7	4.5	4.4
5 Zn (Glass)	3.9	3.6	3.4
<u>5 Zn (comp)</u>	5.1	5.1	4.9
7 Zn (Glass)	4.3	4	3.4
<u>7 Zn (comp)</u>	6	5.8	5.8
10 Zn (Glass)	3.8	3.6	3.5
<u>10 Zn (comp)</u>	5.1	5.1	5
<u>PolyAniline</u>	4.1	4	3.6
<u>Standard Penicillin</u>	2.5	2.8	----
<u>Standard Fluconazole</u>	----	----	3

## 4. Discussion

### 4.1. Interpretation of the collected FTIR spectra

It is found profitable and of much concern to discuss the different collected IR results separately at first for the pure glass and pure polymer (polyaniline) and then moves to the IR results from composite samples.

#### (a) Interpretation IR spectra of base phosphate glass

It is recognized that the identified FTIR spectra reflect the existing structural building units within studied glasses. The vibrational bands in glasses are generally comparable to that usually identified from crystalline analogues except the lack of sharpness. The glasses are considered to be materials of non-periodic arrangements but nevertheless generally

show the same suggested or known structural units from similar crystalline solids. In other words, the vibrational bands obtained from a glass are accepted to be finger-prints of the structural building units in such glass [15-17]. The network structure of all phosphates is known to be dominated by  $PO_4$  tetrahedral and the basic structure of  $P_2O_5$  is modified with the addition of alkali oxide but the phosphorus retains its four-fold coordination throughout the full composition range up to fully alkali oxide saturated orthophosphate. A linear chain is formed upon the addition of a modifier (alkali or alkaline earth oxide) which results in cleavage of the P-O-P linkages and the formation of nonbridging oxygens (NBOs) in the glass structure.

It is evident that the asymmetric and symmetric stretching vibrations characteristics of phosphate units are active in both the IR and Raman spectra. Most previous studies related the vibrational spectra of phosphate glasses to the same assignments of the principal bands known for the normal modes in the vibrational spectra of analogous crystalline phosphates [15-17].

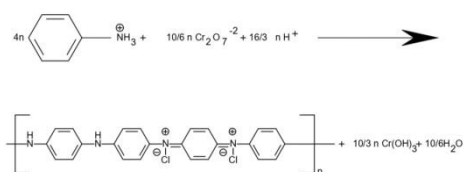
Based on previous published studies [18, 19], the following assignments are recorded for the identified IR spectra from the studied phosphate glasses:

- (i) The peak at  $470\text{ cm}^{-1}$  can be assigned to bending vibrations of P – O – P and the  $PO_2$  modes and also involve sharing vibrations of modifier cations (e.g.  $K^+$ ,  $Ca^{2+}$ )
- (ii) The peak at  $774\text{ cm}^{-1}$  can be attributed to symmetric stretching vibrations of P – O – P linkages.
- (iii) The peaks around 875 and  $1096\text{ cm}^{-1}$  can be attributed to asymmetric stretching vibration of P – O – P units.
- (iv) The absorption peak at  $1273\text{ cm}^{-1}$  can be related to  $PO_2$  vibrations and stretching of the double bond (P=O).
- (v) The near-IR vibrational peaks at 1645 and  $3450\text{ cm}^{-1}$  are related to vibrations of POH, OH and water.

#### (b) Interpretation of the FTIR of polyaniline

For the understanding and explanation of the FTIR spectra of prepared polyaniline by the described method of poly condensation through acidification by HCl solution and oxidation by  $K_2Cr_2O_7$  solution, we refer to the technical report for (IUPAC) published by Trchova and Stejskal [20]. The mentioned authors assumed that the polymerization process procedure adopted by several authors affected the morphology of the polyaniline produced. With strong sulfuric acid a granular morphology was obtained, but in weak acid (acetic) or water, polyaniline nanotubes were produced. The oxidation of aniline under alkaline solution yielded aniline oligomers.

The following sequence of reactions is the most accepted route for the preparation of polyaniline from aniline using HCl and  $K_2Cr_2O_7$  as controlling media as shown in eq. 1 [21].



.... (1)

Different FTIR spectra are expected depending on the way of polymerization. Based on the previous report and other recent published work on related topic by Abdel-salam et al [11,22,23], table (3) summarizes the obtained IR vibrational peaks and their suggested assignments for polyaniline prepared under the same adopted procedure applied in this study.

**Table (3) Peak positions and their proposed assignments [12,22,23]**

Peak position $cm^{-1}$	Assignment
510	Characteristic for transitional oscillation
810	C – H out of plane
1145	*NH= structure formed during protonation
1248	Characteristic of the protonated form and interpreted as C – N <sup>+</sup>
1300	C – N stretching of the secondary aromatic amine
1400	C –N stretching vibrations of $\alpha$ benzoid- quinoid- benzoid sequence
1483	C – C aromatic ring stretching of the benzenoid diamine unit
1565	C = N stretching of the quinoid diamine unit
3480,3520	N – H stretching vibrations

#### (c) Interpretation of the FTIR of the base composite (base glass + polyaniline)

FTIR spectrum of the base composite arises from the combination of both the base glass and polyaniline with a little change in the intensity of peaks. Except for the peak at  $1645\text{ cm}^{-1}$  which is related to the base glass, the rest of peaks are mainly belong to the polyaniline and can be related to their assignments.

#### (d) FTIR of the composite doped with CuO (Cu comp)

It is to be mentioned that not only changing in the intensity of peaks but also shifting from their positions occurred. The presence of CuO as a dopant caused an obvious difference. The peaks are identified at 510, 810, 1145, 1248 and  $1565\text{ cm}^{-1}$

shifted to 503, 800, 1130, 1236 and  $1553\text{ cm}^{-1}$ .

#### (e) FTIR spectra of ZnO-doped composites (Zn Comp)

Adding ZnO in the glass batch as a dopant showed the same effect as in case of CuO. The peaks that showed shifting in their positions in Cu comp samples appeared in the same shifted positions.

#### 4.2. Interpretation of the X-ray diffraction data

The collected X-ray diffraction patterns can be interpreted as follows:

- (i) The base glass and glasses containing dopants of CuO or ZnO reveal no diffraction patterns due to the known randomness or non-periodic structure.
- (ii) The samples containing polyaniline show distinct small diffraction peaks which are related to the formation of salt during the reactions using HCl and  $K_2Cr_2O_7$  solutions leading to the polymeric formation of polyaniline.
- (iii) The composites containing CuO or ZnO showed a little variation in the intensity of peaks which may be attributed to the presence of new phases.

#### 4.3. Interpretation of the SEM data

The morphological textural features identified through SEM measurements for the studied base glass, polyaniline, composites of dopants of CuO or ZnO are explained as follows:

- (i) The images obtained from the base glass show uniform clear background without any indication or appearance of microcrystalline species or features. This result is expected as it is known that glasses are structurally known as non-periodic materials which lack periodicity and described as amorphous materials.
- (ii) The appearance of any scattered pieces or grains in the textures of CuO or ZnO-doped glass can be related to the effect of rinsing of the examined textures with dilute acids or similar solvent during SEM measurements related to separation of micro-grains of divalent oxides or metallic species.
- (iii) The appearance or identification of granular textures in the images of pure polyaniline or composites containing polyaniline can be ascribed to the formation of such granular pieces during the preparation of polyaniline through the adopted method by the use of HCl solution and  $K_2Cr_2O_7$  as oxidant, the same result has been reached by several authors [21, 23, 24].

#### 4.4. Interpretation of the antimicrobial results

The collected measurements shown in table (3) and figure (4) revealed variable responses of the gram positive and gram negative bacteria upon the introduction of the prepared glasses and polyaniline composites. It was reached that the composite derivatives showed the highest antibacterial results. The antimicrobial results can be explained on the following basis:

- (i) The polyaniline is recognized to possess extended branching structure due to polymerization process of its preparation beside granular structure as enhanced and identified by SEM investigations. These features give and acquire higher points of contact between the composite and the microbial species and hence it is expected to be more effective than glasses with non-periodic and non-branching structures.
- (ii) The preparation of polyaniline in the present study is carried out using hydrochloric acid (HCl) solution beside the solution of potassium dichromate ( $K_2Cr_2O_7$ ) as an oxidizing agent. The expected media from such leaching solutions is slightly acidic in nature and this seems to support or initiate the antimicrobial effect. On the other hand, when the pure phosphate glass dissolves in distilled water, it ionizes in acidic phosphate solutions and highly basic KOH beside some  $Ca(OH)_2$  and these mixtures are not indicative for certain direction to control the antibacterial efficiency in continuous direction.
- (iii) Both dopant ions ( $Cu^{2+}$ ,  $Zn^{2+}$ ) have been recognized to be effective in favoring the antimicrobial activity in various glasses [24]. Hence their existence within the compositions of glass, polyaniline or mixed components initiates the antimicrobial activity.
- (iv) Table (3) refers to the prepared composites which are more effective than some used antibiotics such as standard penicillin (antibacterial) and standard fluconazole (antifungal).

#### 5. Conclusions

The present study comprises the preparation of a phosphate glass ( $K_2O-CaO-P_2O_5$ ) by melting-annealing technique and also the preparation of polyaniline through polymerization of aniline by  $K_2Cr_2O_7$  and HCl solutions as an acidic medium. The composite was prepared by combining the glass and the aniline in its monomer form together and then polymerization process occurred through oxidation step using  $K_2Cr_2O_7$  solution.

Multiple characterizations of all the prepared samples were carried out by FTIR, X-ray diffractions

and SEM investigations. Further studies of some selected samples were done to justify their antimicrobial properties.

FTIR spectra of the glass and the derivative doped samples reveal vibrational bands due to stretching and bending of phosphate groups beside vibrations due to modifier cations, OH, POH and water.

FTIR spectra of polyaniline or composite derivatives reveal extended and multi-peaks which are correlated with vibrations of various linkages (e.g. C – N, C – C, C – H).

X-ray diffraction investigations show no distinct patterns from analysis of phosphate glass and doped derivatives. On the other hand, diffraction studies of polyaniline and composite derivatives show 2-3 small peaks which are assumed to be due to salt formation during the polymerization process for the preparation of polyaniline through the action of HCl and  $K_2Cr_2O_7$  solutions.

SEM investigations confirm the amorphicity of the phosphate glass samples and their doped derivatives by showing no evidence of microcrystalline phases. On the other hand, polyaniline and its doped derivatives or composites revealed distinct granular textures which are related to polymerization process during the preparation of polyaniline.

The different studied composites from glass and polyaniline with dopants showed different responses to micro-organisms. In general, they showed high antimicrobial activities against different species of bacteria and yeast. Also, some of the studied composites are superior to the use of standard antibiotics.

#### 6. References

- [1] J. E. Gough, Cartilage tissue engineering, In Tissue Engineering Using Ceramics and Polymers. Woodhead Publishing. (2007) 566.
- [2] E.El-Meliigy, R.van Noort, History, Market and Classification of Bioceramics, In Glasses and Glass Ceramics for Medical Applications. Springer, New York, NY. (2012) 3.
- [3] M. M. Farag, H. S. Yun, Effect of gelatin addition on fabrication of magnesium phosphate-based scaffolds prepared by additive manufacturing system, Materials Letters. 132 (2014) 111.
- [4] J. E. Shelby, Introduction to glass science and technology. Royal Society of Chemistry. (2020).
- [5] M. Dussauze, T. Cardinal, Nonlinear optical properties of glass, In Springer Handbook of Glass. Springer. Cham. (2019) 193.
- [6] S. K. Misra, A. R. Boccaccini, Biodegradable and bioactive polymer/ceramic composite scaffolds, In Tissue Engineering Using Ceramics and Polymers, Woodhead Publishing. (2007) 72.
- [7] H. R. Abd El-Mageed, H. M. Abd El-Salam, M. K. Abdel-Latif, F. M. Mustafa, Preparation and spectroscopic properties, density functional

- theory calculations and nonlinear optical properties of poly (acrylic acid-co-acrylamide)-graft polyaniline, *Journal of Molecular Structure*. 1173 (2018) 268.
- [8] E. M. S. Azzam, H. M. Abd El-Salam, R. S. Aboad, Kinetic preparation and antibacterial activity of nanocrystalline poly (2-aminothiophenol), *Polymer Bulletin*. 76 (2019) 1929.
- [9] G. Bereket, E. Hür, Y. Şahin, Electrochemical synthesis and anti-corrosive properties of polyaniline, poly (2-anisidine), and poly (aniline-co-2-anisidine) films on stainless steel, *Progress in organic coatings*. 54 (2005) 63.
- [10] S. Sathiyarayanan, S. Devi, G. Venkatachari, Corrosion protection of stainless steel by electropolymerised pani coating, *Progress in organic coatings*. 56 (2006) 114.
- [11] H. M. Abd El-Salam, G. M. Abd El-Hafez, H. G. Askalany, A. M. Fekry, A Creation of poly (N-2-hydroxyethylaniline-co-2-chloroaniline) for corrosion control of mild steel in acidic medium, *Journal of Bio-and Tribo-Corrosion*. 6 (2020) 14.
- [12] K. P. Jotiram, R. G. S. V. Prasad, V. S. Jakka, R. S. L. Aparna, A. R. Phani, Antibacterial Activity of Nanostructured Polyaniline Combined With Mupirocin, *Nano Biomedicine & Engineering*. 4 (2012) 144.
- [13] P. Boomi, H. G. Prabu, Synthesis, characterization and antibacterial analysis of polyaniline/Au-Pd nanocomposite, *Colloids and Surfaces A: Physicochemical and Engineering Aspects*. 429 (2013) 51.
- [14] V. Mishra, D. N. Prasad, Application of in vitro methods for selection of *Lactobacillus casei* strains as potential probiotics, *International journal of food microbiology*. 103 (2005) 109.
- [15] P. H. Gaskell, Glass: Structure by Spectroscopy, *Physics Bulletin*. 28 (1977) 574.
- [16] A. Abdel-Kader, A. A. Higazy, M. M. Elkholy, Compositional dependence of infrared absorption spectra studies for  $\text{TeO}_2\text{-P}_2\text{O}_5$  and  $\text{TeO}_2\text{-P}_2\text{O}_5\text{-Bi}_2\text{O}_3$  glasses, *Journal of Materials Science: Materials in Electronics*. 2 (1991) 157.
- [17] A. M. Efimov, IR fundamental spectra and structure of pyrophosphate glasses along the  $2\text{ZnO} \cdot \text{P}_2\text{O}_5\text{-}2\text{Me}_2\text{O} \cdot \text{P}_2\text{O}_5$  join (Me being Na and Li). *J. non-cryst. solids*. 209 (1997) 209.
- [18] A. M. Fayad, M. A. Ouis, F. H. ElBatal, H. A. ElBatal, Shielding Behavior of Gamma-Irradiated  $\text{MoO}_3$  or  $\text{WO}_3$ -Doped Lead Phosphate Glasses Assessed by Optical and FT Infrared Absorption Spectral Measurements, *Silicon*. 10 (2018) 1873.
- [19] M. A. Ouis, M. A. Azooz, H. A. ElBatal, Optical and infrared spectral investigations of cadmium zinc phosphate glasses doped with  $\text{WO}_3$  or  $\text{MoO}_3$  before and after subjecting to gamma irradiation, *Journal of Non-Crystalline Solids*. 494 (2018) 31.
- [20] M. Trchová, J. Stejskal, Polyaniline: The infrared spectroscopy of conducting polymer nanotubes (IUPAC Technical Report), *Pure and Applied Chemistry*. 83 (2011) 1803.
- [21] M. S. Zoromba, S. Alghool, S. M. S. Abdel-Hamid, M. Bassyouni, M. H. Abdel-Aziz, Polymerization of aniline derivatives by  $\text{K}_2\text{Cr}_2\text{O}_7$  and production of  $\text{Cr}_2\text{O}_3$  nanoparticles, *Polymers for Advanced Technologies*. 28 (2017) 842.
- [22] M. Trchová, I. Šeděnková, E. Tobolková, J. Stejskal, FTIR spectroscopic and conductivity study of the thermal degradation of polyaniline films, *Polymer Degradation and Stability*. 86 (2004) 179.
- [23] T. Abdiryim, Z. Xiao-Gang, R. Jamal, Comparative studies of solid-state synthesized polyaniline doped with inorganic acids, *Materials Chemistry and Physics*. 90 (2005) 367.
- [24] H. A. ElBatal, A. A. El-Kheshen, N. A. Ghoneim, M. A. Marzouk, F. H. ElBatal, A. M. Fayad, A. A. El-Beih, In vitro bioactivity behavior of some borophosphate glasses containing dopant of  $\text{ZnO}$ ,  $\text{CuO}$  or  $\text{SrO}$  together with their glass-ceramic derivatives and their antimicrobial activity, *Silicon*. 11 (2019) 197.